Functionalized microfibers for field-responsive materials and biological applications

G Bossis, J Alves-Marins, P Kuzhir, O Volkova, A Zubarev

Functionalized microfibers for field responsive materials and biological applications

G.Bossis[1], J.Alves-Marins[1], P.Kuzhir[1], O.Volkova[1], A.Zubarev[2]*[1]CNRS, UMR7336, Laboratoire de Physique de la Matière Condensée, Université de Nice-Sophia Antipolis, 28 avenue Joseph Vallot, 06100 Nice, France*

[2]Urals Federal University, Lenina Ave 51, 620083, Ekaterinburg, Russia

Introduction

Electrorheological (ER) and Magnetorheological (MR) are suspensions of micro or nanoparticles which can be easily polarized by the application of respectively an electric or a magnetic field.The dipolar interaction between the particles make them to aggregate in a solid network which gives to the suspension the properties of a solid. The main characteristic of this solid state is its yield stress which can reach quite easily 50kPa with MR fluids and usually only a few kPz for ER fluids, expect for a given class called giant electrorheological fluids (GER) which can overcome 100kPa although the reproducibility and practical use of these new fluids is still under test. Conventional ER and MR fluids are made of micronic or slightly submicronic spherical particles and ,due to their size they sediment quite quickly and can definitively remain aggregated in the absence of remixing during a long period. These last years it was found that fiber like particles can present two main advantages on spherical ones: a higher yield stress for the same volume fraction and applied field and a much lower sedimentation rate (Yinet al., 2006; Bell et al., 2007, 2008; Lopez-Lopez et al., 2007; Vereda et al., 2007). The reason for a lower sedimentation rate stands in the formation of a percolated network at low volume fraction which is strong enough to prevent its compaction. On the other hand the fact that the yield stress of a field induced network made of fibers is much lager than the one made of spheres has no clear explanation. A possible one could be related to the rôle of friction since the deformation of a network of fibers will involve the sliding of fibers along each other . A theoretical approach of this sliding friction was previously

explored (Lopez-Lopez et al., 2009). In this paper we shall compare the prediction of this theory to experimental results obtained with fibers both in magnetorheology and electrorheology. We shall pay attention to the comparison between frictional effect on one hand and enhancement of local torque and rupture forces coming from the elongated shape on the other hand.

The first part will be devoted to a short description of the macroscopic model which considers the friction forces induced by the magnetic torque on the aggregates; we shall emphasize the role of the different parameters which are the friction parameter, ξ, the internal volume fraction of the aggregates, ϕ_a, and the orientational order of the fibers relatively to each other. A comparison between experiments on magnetic fibers and magnetic spheres will be discussed in the light of the macroscopic model and also of results obtained on the rupture force between two macroscopic fibers.

In the second part we shall adress the case of sepiolite fibers fuctionnalized with a conductive polymer, namely polyaniline, and we shall compare the ER effect obtained with a suspension made of pure PANI fibers to the one of a suspension made of sepiolite coated with PANI. The difference between these two kinds of fiber being essentially their shape factor, we shall show how this shape factor determines the yield stress of the suspension.

I-1 Theoretical approach for including friction in the yield stress of MR or ER

This approach was developped in (Kuzhir et al., 2009) and we shall just recall the main steps which will be usefull for the further investigation. In the so-called macroscopic approach we relate the yield stress to the torque on aggregates of particles filling the cell. This theory was developped for aggregates of spheres (Bossis et al,1997) but can be easily adapted for aggregates of fibers. An important parameter of the model is the internal volume fraction Φ_a

inside the aggregates, which should not be confused with the average volume fraction Φ . Inside the aggregates we assume that the fibers have a certain part in contact with each other as represented in Figure 1.

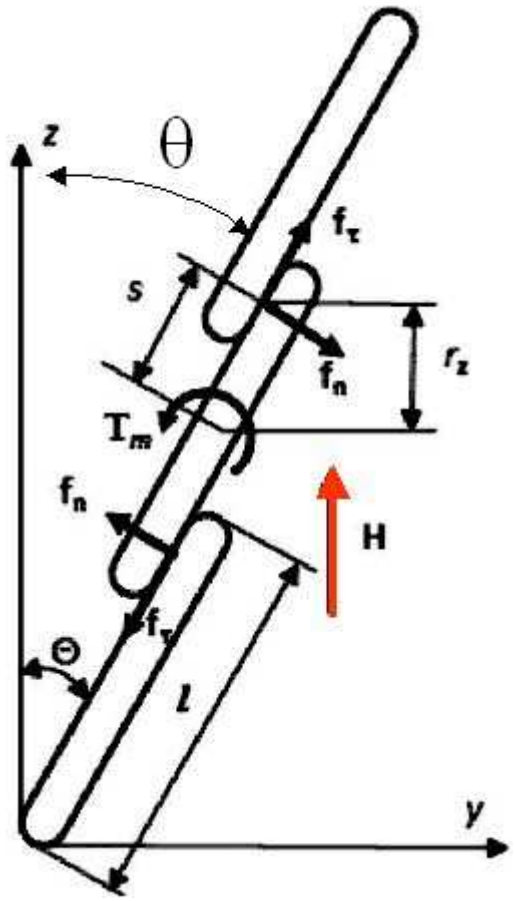

Figure 1. Schematic representation of contact

Each fiber considered independently is subjected to a magnetic torque :

$$T_m = \vec{m} \wedge \vec{H} = m_{\perp} H_{\parallel} - m_{\parallel} H_{\perp} \qquad (1)$$

Where H is the average magnetic field in the sample and m the magnetic moment of the fiber the notations // and $\perp$ are respectively to the parallel and perpendicular directions to the axis of the fiber (Fig.1). The average field inside the fiber is just $H_f^{\parallel}$=Hcos(θ) since the depolarization factor is close to zero for an elongated cylinder.On the contrary the perpendicular field inside the fiber depends on the demagnetization factor which we take equal to 0.5 for high aspect ratio, then we have from a mean field theory:

$$H_f^{\perp} = H_{\perp}(1+\frac{\chi_{\perp}}{2})/(1+\frac{\chi_p}{2}) \qquad (2)$$

where $\chi_{\perp}$ is the average susceptibility of the suspension in the y direction and χ_p the intrinsic suceptibility of the particle material that we shall approximate by the Frolich-Kennelly law:

$$\chi_p(H) = \frac{\chi_i}{1+\frac{\chi_i H}{M_s}} \qquad (3)$$

with χ_i the initial susceptibility and M_s the saturation magnetization.

Setting in (1) : $m_{\perp} = \chi_p H_{\perp}^f$ and $m_{\square} = \chi_p H \cos(\theta)$ and using (2) we end up with:

$$T_m = \mu_0 V_f \, H^2 \chi_p^2 \frac{(1-\Phi)}{2+\chi_p(1-\Phi)} \sin(\theta)\cos(\theta) \qquad (4)$$

Where V_f is the volume of the fiber. Note that for Φ=1 the torque cancels because there is no more place for shape anisotropy , but at low volume fraction, the magnetic torque becomes independent of the neighbour particles.

The tangential stress is :

$$\sigma_{yz} \equiv \tau = \frac{1}{V} \sum r_z f_y \qquad (5)$$

Where f_y is the component along the y direction of the contact force of a reference fiber with its neighbour (Figure 1). This force is a reaction force fn normal to the fiber axis and related to the magnetic torque by $f_n=T_m/2s$ with 2s the distance between the two contact points. The friction forca can be introduced at this point since it is proportional to the normal force and directed along the fiber axis (f_τ in FIg.(1)). Therefore the force f_y in (5) is given by:

$$f_y = \frac{T_m}{2s}\cos(\theta) + \xi \frac{T_m}{2s}\sin(\theta) \qquad (6)$$

Combinig (5) and (6) and noting that r_z=s cos(θ) we obtain the following shear stress

$$\tau(\theta) = \frac{\Phi}{\Phi_a} \mu_0 H^2 \frac{\chi_a^2 (1-\frac{\Phi}{\Phi_a})}{2+\chi_a(1-\frac{\Phi}{\Phi_a})} \frac{\sin(2\theta)}{2} \left[\cos^2(\theta) + \xi \frac{\sin(2\theta)}{2} \right] \qquad (7)$$

This expression takes into account that the fibers gather inside aggregates of internal volume fraction Φ_a ; for individual chains of fibers we should have to put Φ_a=1 and to replace χ_a by χ_p. For ferromagnetic particles the intrinsic suceptibility is high and so is the suseptibility of the aggregates, so the order of magnitude of the yield stress is:

$$\tau \approx \chi_a(H)\Phi\mu_0 H^2 \qquad (8)$$

It appears that the main quantity which determines the magnitude of the yeild stress is the magnetic susceptibility χ_a of the aggregates. In the next section we are going to see what is the difference of susceptibility between aggregates of fibers and aggregates of spheres.

I-2-Magnetic susceptibility of aggregates

In order to determine the magnetic susceptibility of the aggregates we shall use the extension of the Maxwell-Garnett theory to the case of ellipsoidal particles. This theory predicts the following equation for the susceptibility of an isotropic suspension of fibers:

$$\chi_{a\_i} = \frac{(\beta_{//} + 2\beta_{\perp})\Phi_a}{1-(n_{//}\beta_{//} + 2n_{\perp}\beta_{\perp})\Phi_a} \qquad (9)$$

with $\beta_{\square} = \frac{1}{3} \quad \frac{\chi_p}{1+n_{\square}\chi_p}$ and $\beta_{\perp} = \frac{1}{3} \quad \frac{\chi_p}{1+n_{\perp}\chi_p}$ (10)

The combination $\beta_{//} + 2\beta_{\perp}$ stands for an isotropic medium; if all the fibers are aligned ,we shall have instead $3\beta_{//}$ and equation (9) will read:

$$\chi_{a\_a} = \frac{3\beta_{//}\Phi_a}{1-3n_{//}\beta_{//}\Phi_a} \qquad (11)$$

The quantities $n_{//}$ and $n_{\perp}$ are the well known demagnetisation factors which, for a revolution body, satisfy the relation $n_{\perp} = (1-n_{\square})/2$. For spheres $n_{//}=n_{\perp}=1/3$ whereas for needles $n_{//}=0$ and $n_{\perp}=1/2$. The equation 9 applies whatever the aspect ratio is. In Figure 2 we have plotted the ratio of the susceptibility of aggregates of fibers divided by the suceptibility of aggregates of spheres having the same volume fraction $\Phi_a=0.6$ for the cases of aligned fibers and isotropicall oriented fibers. We have chosen an aspect ratio of 10 . The magnetic susceptibility of cobalt is represented by equation 3 with $\chi_i=70$ and $M_s=1370$kA/m. We see that replacing fibers by spheres, we have a large increase of the magnetic susceptibility, especially at low field. On the other hand this increase depends a lot on the orientational

order, since we can see that at low field the increase is two times more for aligned fibers than for disoriented fibers.

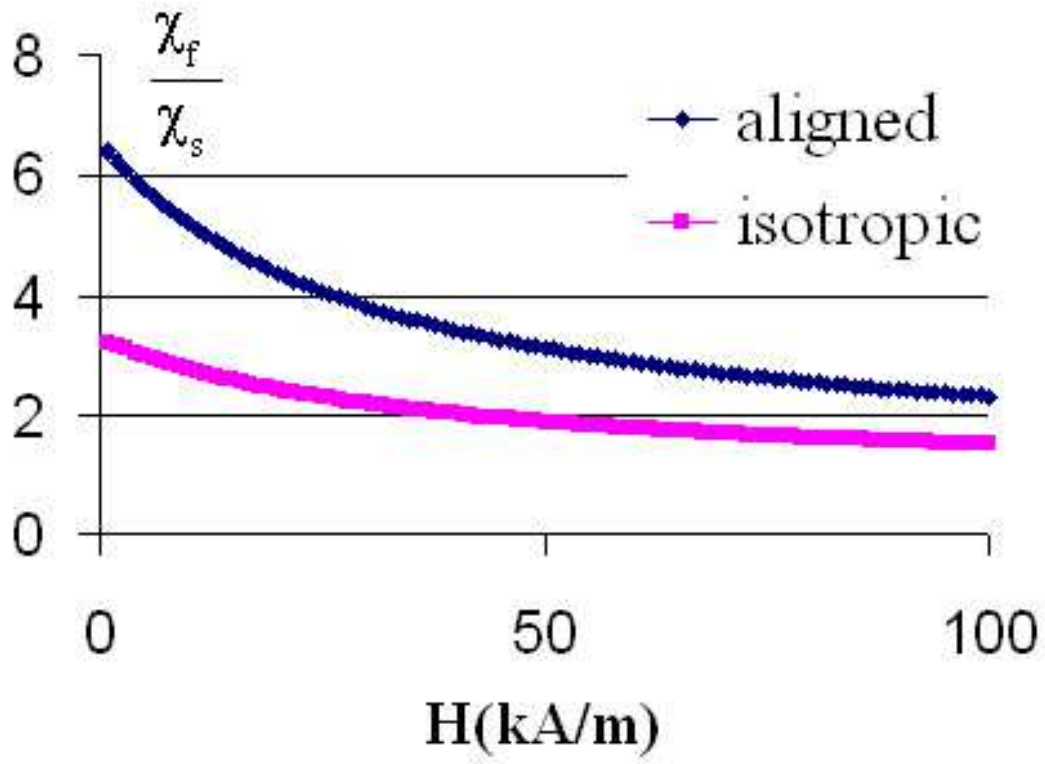

Figure 2. Ratio of the susceptibilities of aggregates of cobalt fibers to aggregates of cobalt spheres at volume fraction Φ_a=0.64 and for aspect ratio r=10.Upper curve: fibers aligned in the field directtion; lower curve:fibers randomly oriented

We are now going to see how it compare with experimental results that we obtained for a suspension of cobalt fibers (Lopez-Lopez et al., 2009).

I-3 Comparison with experiments for cobalt microparticles

The experimental results that we are going to use for this comparison were obtained with cobalt rods of average length of 60 ± 24 μm and diameter 4.8 ± 1.9μm, so an average aspect ratio r=12. The average diameter of the cobalt spheres was $d=1.34 \pm 0.4$ μm.

The yield stress is obtained by finding the maximum of t(q) . If the friction coefficient is zero this angle is equal to 30° and it increases slightly with ξ; for insrance it is equal to 37° if ξ=0.4. In fig.3 we have reported the comparison between the experimental curves and the theoretical ones calculated with the help of equations (7) and (11) corresponding to aligned

fibers. Besides the degree of alignment there are two unknown variables: the internal volume fraction Fa and the value of the friction coefficient x. We can see in Figure 3 that we can obtain a good agreement between experiment and theory for the yield stress of fibers either with ξ=0.4 and Φ_a=0.5 or with ξ=0 and Φ_a=0.64, this last value corresponding to the random packing of spheres.

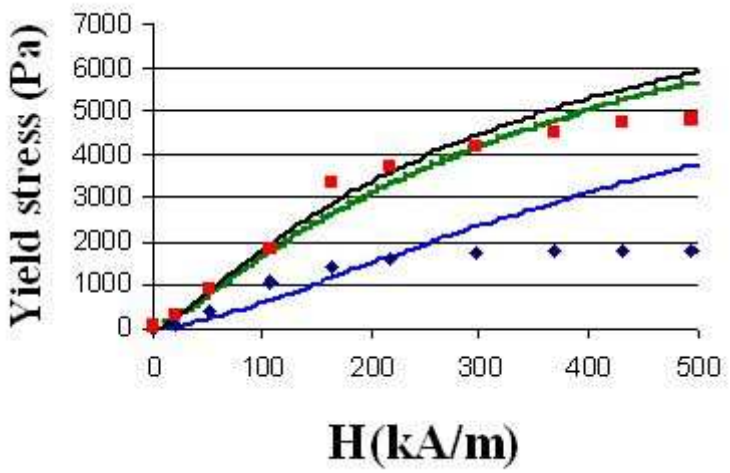

Figure 3. Yield stress versus magnetic field for a volume fraction Φ=0.05. theory for fibers (ξ=0.4,Φ_a=0.5) ; theory for fibers (ξ=0.,Φ_a=0.64) ; : theory for spheres: (ξ=0.,Φ_a=0.64); experiments for fibers; ◆ ◆ experiments for spheres

The prediction of the model for spherical particles uses ξ=0 because we do not expect too much friction between spherical particles. As for the experimental curve the prediction is well below the one for fibers, but it does not show the saturation observed in experiments. This could be due to the fact that,as already emphasized, the critical angle where $\tau(\theta)$ passes through a maximum does not depend on the field if there is no friction. Aggregates composed of fibers can easily deform through slipping between fibers, this is more difficult for aggregates of spheres and it is understandable that the stronger are the magnetic interactions the smaller will be the rupture angle and so the yield stress. The main information that we can draw from this comparison is that the increase in yield stress for suspension of fibers is mainly due to the increase of the permeability of aggregates, but that it is difficult to assess the rôle of friction since we do not know the internal volume fraction of fiber aggregates, nor the orintation of the particles inside the

aggregates. An illustration of these aggregates for spindle like iron particles coated with silica (Mendez-Garza et al., 2013) is represented in Figure 4. We see fist the fact that particles separate in well individualized aggregates and, second that the volume fraction inside the aggregates seems quite large, but difficult to evaluate; also the orientational order is far to be perfect, although closer to fully aligned than to randomly oriented.

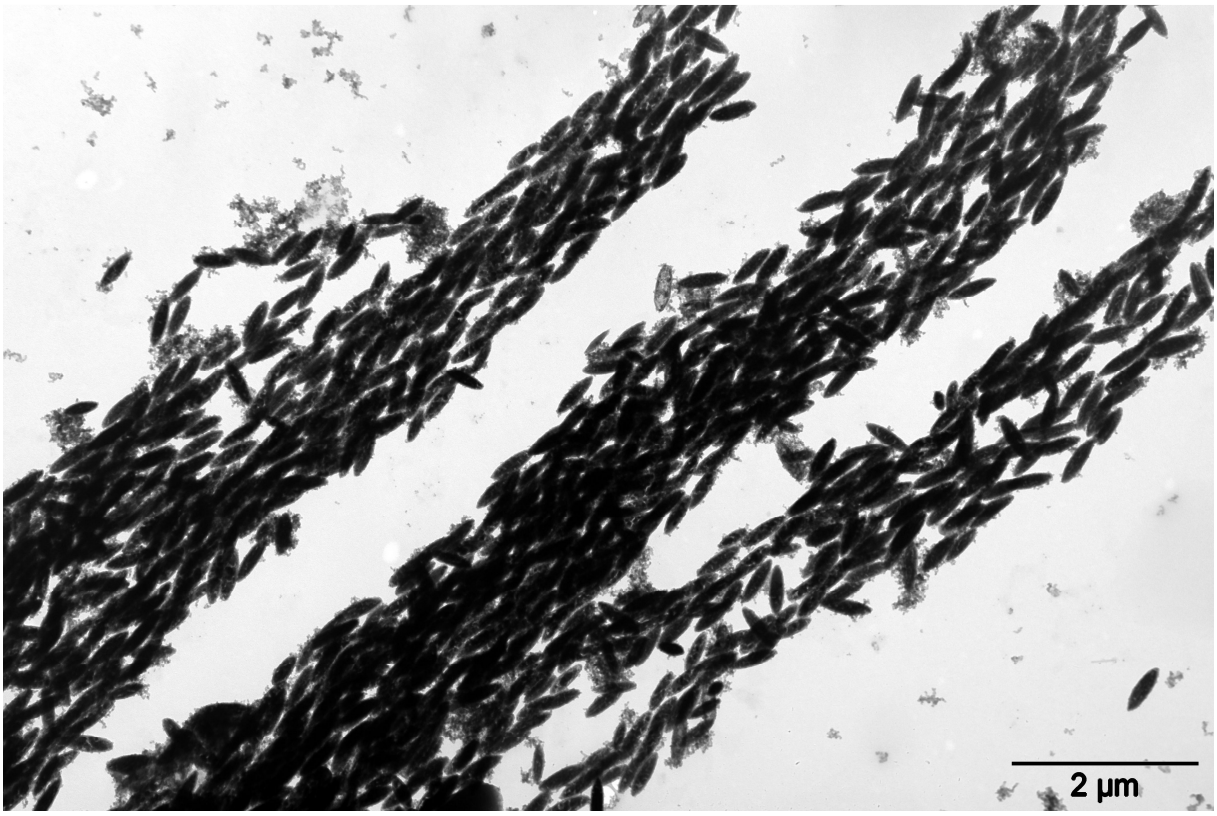

Figure 4. TEM image of iron nanoparticles coated with silica dried in the presence of a magnetic field

Until now our model and discussion was based on the so called "macroscopic model of yield stress" (Bossis et al., 1997) which supposes that all the resistance to the deformation of the suspension under shear stress comes from the macroscopic torque exerted on the aggregates, but in a different approach -more valid at high volume fraction where individual aggregates do not exist- we can calculate the yield stress from the rupture between pairs of particles(this is the standard chain model in magnetorheology (Ginder et al., 1996). It can give quite correct predictions (Bossis et al., 2002) and so, it is interesting to compare the rupture forces between spheres and cylinders having the same volume

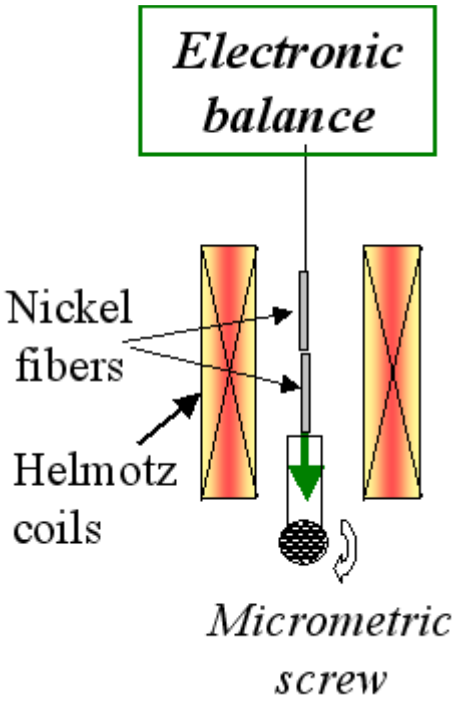

Figure 5. Schematic view of the device

. A schematic view of the experiment is represented in Figure 5 which is similar to the one used by (Volkova, 1998), The upper nickel cylinder (from Goodfellow with diameter 2mm) is suspended to an electronic balance. The lower cylinder is attached to a micrometric screw and the two fibers are placed at the center of a pair of Helmotz coils. The fibers are brougth into contact under magnetic field until the balance indicates a zero weigth, then the fiber is pulled down with the micrometric screw and we record the maximum of the force which corresponds to the rupture force. Furthermore the extremity of the cylinder can be flat or hemispherical, so we have three situations for the end to end configuration: plane-plane; sphere-plane and sphere-sphere. The aspect ratio was r=10. For the spheres we have used chains of 10 spheres inside an aluminium container perced with a small hole such that a part of the first sphere is outside of the container;also the rupture force was multiplied by the ratio of the volume of the cylinder to the volume of the chain in order to keep the same volume fraction. The results are presented in figure 6 for the rupture force versus the applied field. First we see that the larger rupture force is obtained between two cylinders with flat ends and that either with sphere -plane or sphere -sphere extremities the force decreases by almost a factor of two. The rupture force between two chains of spheres is still much lower ,especially at low field. At last we see that the rupture force between two spheres alone is still lower than the one of a chain of sphere,effect which is due to a partial decrease of the demagnetisation factor when we have a chain of spheres. This difference was expected on the basis of finite element calculation at small -but non zero- separation done by (De Vicente et

al., 2010) although the comparison done between chains of spheres and spherocylinders was showing a much smaller difference than our experimental results.

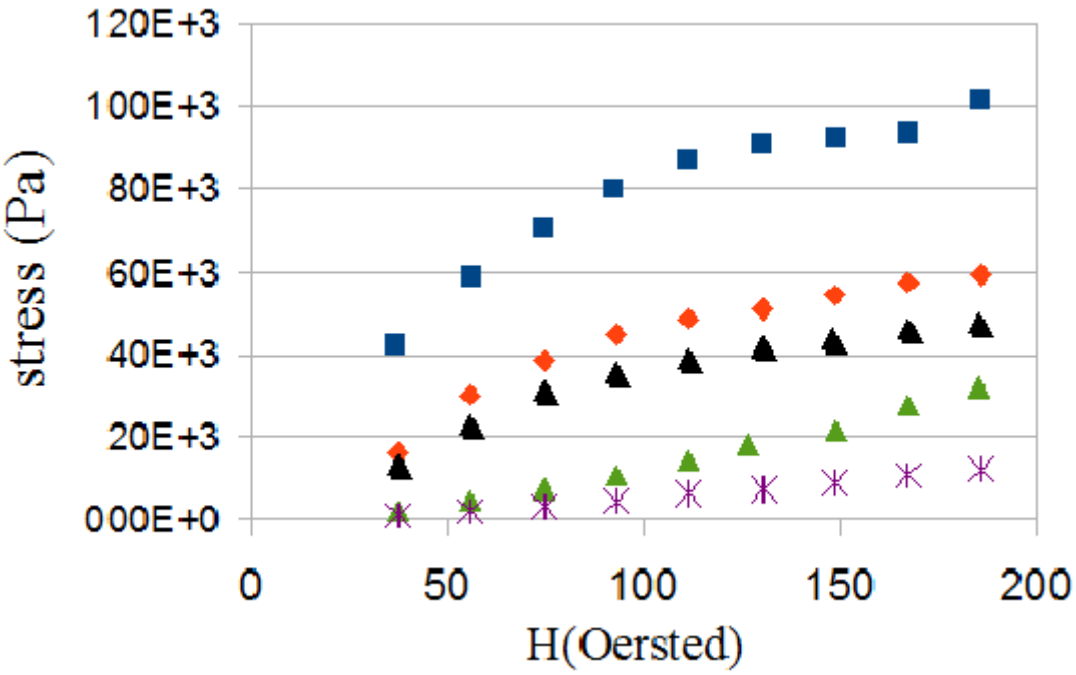

Figure 6. Rupture stress between fibers and chains of spheres with aspectr ratio r=10

■ ■ 2 cylinders with flat ends; ◆◆◆ cylinder with flat end and spherocylinder; ▲▲▲: 2 spherocylinders; ▲▲▲: 2 Chains of 10 spheres ✳✳✳: two spheres

To summarize this comparison between spheres and fiber particle shape in MR suspensions, we can conclude that the main reason for the higher yield stress observed in these fluids come from the higher magnetic permeability of the aggregates of particles because of the decrease of the demagnetisation factor. This higher magnetization is also the reason for the higher rupture stress that we have observed experimentally on a two body experiment. On the other hand friction likely also contributes, but its importance is difficult to evaluate quantitatively because too many parameters are unknown like the internal volume fraction of the aggregates, the value of the friction coefficient and the orientation of the fibers inside the aggregates. It is nevertheless worth stressing that, if the fiber shape is interesting to reduce the sedimentation and the aggregation and at the same time to increase the stress, the volume fraction will hardly

overcome 10% due to the strong enhancement of the viscosity with the aspect ratio which is a general feature of such suspensions (Larson, 1999).In the following section we are going to discuss results obtained with suspension of fibers ,but this time for their use in ER fluids.

II- Use of coated fibers in electrorheological fluids

Most of the particles used to prepare anhydrous ER fluids have either a high dielectric permittivity and/or a coating which strongly enhance the polarizability of the coated particles. For instance the enhancement of the permittivity produced by the alignment of polar molecules on the direction of the local field inside the gap between particles is believed to be the cause of the giant electrorheological effect (Wen et al., 2003; Wu et al., 2012). Among the different coating, the one using a conducting polymer like polyaniline, copolyaniline and polypyrrole (Kim et al., 2002) is often used since it increases the effective permittivity without giving electric breakdown as with metal particles. Polyaniline (PANI) presents good electrical conductivity, which can be controlled through the pH value, easiness of preparation and relatively low density, thus reducing their sedimentation rate; furthermore this is one of the cheapest conducting polymer material (Anilkumar et al., 2006). Nevertheless the yield stress, obtained with these particles remained quite low, likely due to the too high current density of the corresponding fluids (Liu et al., 2011). In order to reduce the conductivity it was proposed to coat polyaniline on inorganic particles or insulating polymer. (Choi et al., 2001; Lim et al., 2002 and Song et al., 2008) prepared PAni/Clay composites, which presented irregular morphology and better ER effect. We have used as a support for PANI a kind of clay called sepiolite which is a clay composed of hydrated magnesium silicates. Interestingly this clay is formed of fibers with a quite large aspect ratio (1-5 μm in length and 20-40 nm in diameter) and with silanol groups on their surface which allow building hydrogen bonding with PAni without the needs to add compatibilizing agent. Like in the magnetic case, the dipole moment is larger for elongated particles than for spherical particles

of the same size and polarizability (Ramos-Tejada et al., 2009) so we expect a higher yield stress than with other pure PANI fibers, both due to the intermediate value of their conductivity which prevents electric breakdown and to their elongated shape. In a previous work (Marins et al., 2013) we described the synthesis of PANI/sepiolite hybrid particles and presented first results showing the improvment of ER properties of these fluids compared to previous results on PANI based fluids experimental results. In the following we are going to complete the experimental results presented elsewhere and to analyse them in the frame of the complex permittivity model extended to the case of fibers.

. III-1 Experimental results

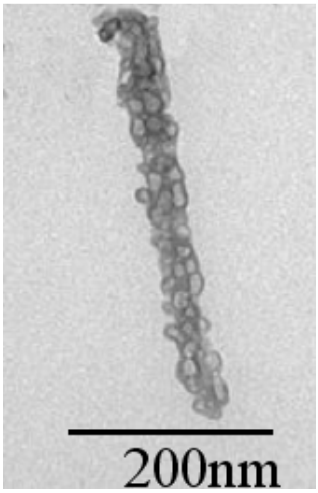

Figure 7a. Hybrid

Figure 7b. Pure PANI

In Figure 7a and Figure7b are representative TEM pictures of respectively the composite PANI/sepiolite (which was composed of 46% in mass of PANI and 54% of sepiolite)and pure PANI fibers. It is interesting to note that the coating of PANI on sepiolite was not homogeneous but rather made of clusters which likely form a percolated network at the surface of the particle. The conductivity (deduced from the measurement on a compressed powder at a volume fraction of 65%) of the hybrid sepiolite-PANI particles was $\sigma_{SP}=2\ 10^{-7}$ S/m compared to the one: $\sigma_P=7.3\ 10^{-6}$ S/m of the Pure PANI particles measured in the same condition .This large difference of conductivity indicates that the network of PANI clusters at the surface of the particles is rather loosely connected. The average aspect ratio of the hybrid was r=25 for the hybrid against r=8 for pure PANI. The corresponding values of the yield stress and shear modulus measured at different rms values of the electric field are presented respectively in

Figures 8 and 9 for the same volume fraction: Φ=10%. The frequency of the applied field was ν=10Hz.

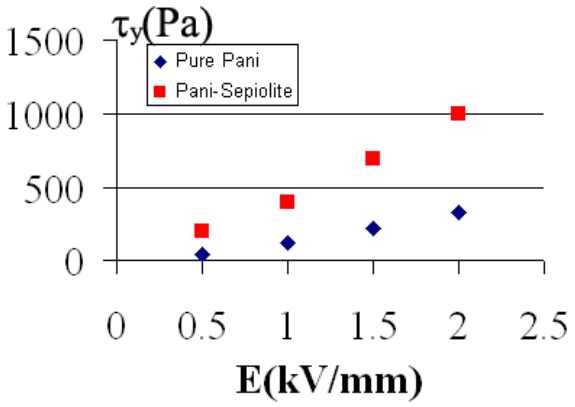

Figure 8. Yield stress versus electric field for a

For the yield stress the ratio between the hybrid and pure PANI is between 6 at low field and 3 at high field in favor of the hybrid composite and for the shear modulus this ratio is almost constant and around 10. These results show how efficient is the coating of the sepiolite to increase the electrorheological efficiency, and this is particularly true for the shear modulus since it increases by an order of magnitude and reaches 600kPa at a moderate field of 2kV/mm which competes with the increase of modulus obtained with magnetorheological fluids.

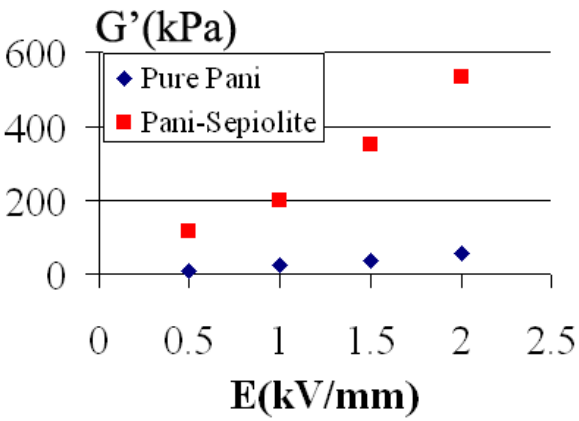

Figure 9. Shear modulus versus rms amplitude of the electric field at a strain

In order to understand what are the reasons of this improvment we have to compare the dipolar forces induced by the interface polarization in the two cases:pure PANI and hybrid particles.

III-2 Dipolar model for forces between elongated particles

The dipolar forces between two spherical particles when there is a mismatch in conductivity and permittivity between the particles and the fluid is expressed as:

$$F \propto (\beta E_0)^2 \quad \text{with} \quad \beta = \frac{K_p^* - K_f^*}{K_p^* + 2K_f^*} \qquad (12)$$

The complex permittivity is $K_p^* = \varepsilon_p - \frac{i\sigma_p}{\omega}$ and similarly for K_f^* (C.W.Wu et al,1997).

The generalization to ellipsoïdal particles is straightforward and reads (T.B.Jones,1995):

$$\beta_\alpha = \frac{K_p^* - K_f^*}{3\left[K_f^* + (K_p^* - K_f^*)n_\alpha\right]} \qquad (13)$$

The indice α denotes the axis relatively to the principal axes of the particle. In practice we shall consider that the particles are aligned on the field and α corresponds to the parallel case. The dipolar force is proportional to the modulus of the equation (13):

$$F \propto \left|\beta_{//}^2\right| E_0^2 = \frac{1+(\omega\tau_0)^2}{1+(\omega\tau_{MW})^2}\left(\frac{\sigma_p - \sigma_f}{3\left[\sigma_f(1-n_{\square}) + \sigma_p n_{\square}\right]}\right)^2 E_0^2 \qquad (14)$$

Where $\tau_{MW} = \frac{(1-n_{\square})\varepsilon_f + n_{\square}\varepsilon_p}{(1-n_{\square})\sigma_f + n_{\square}\sigma_p}$ is the Maxwell Wagner interfacial polarization time related to the parallel axis and $\tau_0 = \frac{\varepsilon_p - \varepsilon_f}{\sigma_p + \sigma_f}$

Equation (14) describes the linear case where there is no limitation on the value of the local electric field in the gap between two particles. In practice there is a maximum field E_m due to the ionization of the molecules, and in a certain zone between the particles the local field can't exceed E_m (Gonon et al., 1999). Taking into consideration this limitation on the field, the force between two spherical particles can be calculated and show a weaker power law as the classical E^2 . The generalization of this theory to the case of ellipsoidal or cylindrical particles was not done to our knowledge, but for the sake of comparison between two kinds of particles we shall assume that the ratio of the linear polarization forces (equation(14)) will give the right order of magnitude. The permittivity and conductivity of the suspensing silicone oil are respectively ε_f=3.8 ε_0 and σ_f=10^{-10}S/m . The conductivity and permittivity measured on

pellets at a frequency of 10Hz are for the pure PANI: ε_p=1128 ε_0 and σ_p=7.3 10^{-6}S/m and for the hybrid particle: : ε_p=137 ε_0 and σ_p=2 10^{-7}S/m . With these values the ratio of the dipolar forces calculated with the help of Equation (14) give F_{hybrid}/F_{Pani}=5 which is actually the right order of magnitude since the the ratio of yield stress was varying between 6 and 3 at the higher field ,knowing that the linear theory becomes worse when the applied field increases. In the synthesis it is possible to increase or decrease the proportion of PANI relatively to the sepiolite and this will change both the conductivity and the permittivity of the hybrid particles. We have plotted in Figure10 the ratio F_{hybrid}/F_{Pani} versus the conductivity of the hybrid particle, for three different values of the permittivity of the hybrid composite since we do not know, a priori, the relation between the conductivity and the permittivity when we increase the PANI weight fraction. The lower curve correspond to the experimental permittivity; ε_{hybid}=137 and the ratio of forces is equal to 5 for the experimental conductivity σ_{hybrid}=2 10-7.

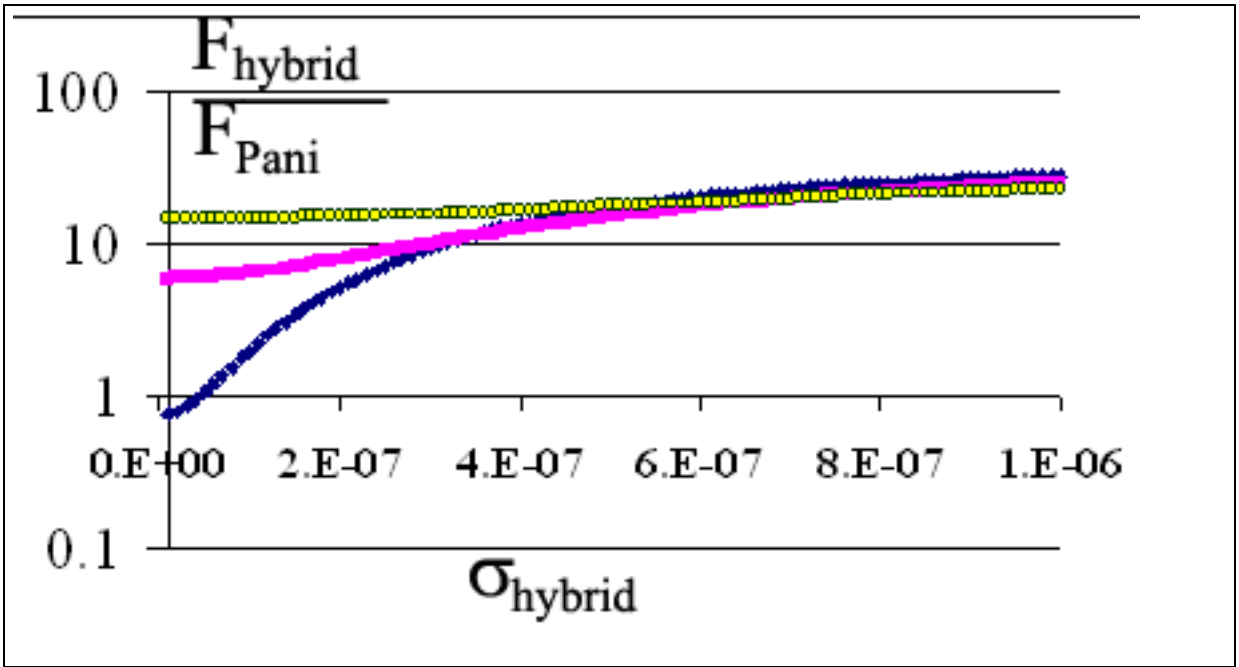

Figure 10. Ratio of the interparticle force (Eq.(14)) betwwen hybrid particlesto the one between pure Pani particles versus the conductivity of the hybrid particle for three values of permittivity: _____ ε_{hybrid}=137; _____ ε_{hybrid}=548; _____ ε_{hybrid}=1370

We see that increasing the conductivity of the hybrid, increase strongly the ratio of forces,that is to say the ratio of yield stresses, and that it is true whatever the increase of premittivity is. The liliting value corresponding to the conductivity of pure PANI is a ratio of 36. This stress enhancement is then the one resulting uniquely of the increase of aspect ratio between the hybrid and the pure PANI. Of course there is a compromise to find on the weight proportion of PANI with respect to sepiolite since a too high conductivity limits the local field betwwen the particles and reduces the yield stress, but from this calculation, just increasing the conductivity of the hybrid by a factor of two would already give a yield stress enhancement of 13.5 compared to pure PANI.

IV- Conclusion

We have seen that the use of elongated , fibers like particles, was interesting in order to increase the magnetorheological or the electrorheological response of the suspensions made with these fibers when compared to suspensions of spheres at the same volume fraction. The main cause, of this improvment is the increase of the polarization of the particles due to their elongated shape. This does not rule out the effect of friction, but without a better knowledge of the internal structure of the aggregates of particles, it is not possible to quantify its contribution to the yield stress. For mineral fibers covered with a conducting polymer we also observe a large improvment of the yield stress and shear modulus which can be asssociated to the larger aspect ratio of this hybrid particle. The model predicts that it could be still increased several times if the conductivity of this hybrid particle was the one of the pure PANI, but likely a too high conductivity would provoke an ionization of the fluid and a limitation of the local field so that a compromise should be found at some intermediate value of the coverage ratio. New synthesis with coverage ratio larger than 46% should be realized in order to test this hypothesis. It is also worth noting that the improvment on yield stress or shear modulus that is obtained by using elongated particles instead of spherical ones is limited

to low to intermediate volume fraction (typically below 5%-20% depending on the aspect ratio, r). This is because the intrinsic viscosity of a suspension of fibers can increase steadily when we enter in the semi dilute regime ($\phi_0 \approx 24\, r^2$) especially if their Brownian motion remains important (Larson R.G, 1998) and for most of the applications we need a low viscosity in the absence of applied field.

We have seen that mineral fibers , like sepiolite, can be quite easily functionalized thanks to their silanol group on their surface. It is possible , for instance, to graft magnetite nanoparticles on their surface , in order to obtain magnetic fibers with a large aspect ratio and a much lower density than those made of bulk iron ,nickel or cobalt. These magnetic fibers with a large aspect ratio can be used as fillers to reinforce, for instance, epoxy resins with the advantage to be able to orient the fibers before polymerization and so to reinforce the material in the direction where it will be submitted to the higher stress (Alves Marins et al, submitted).Besides mechanical applications, magnetic nano or microfibers can be used for biological apllications. For example their vibration induced by a magnetic field when they are adherent to the membranes of cancer cells can create large pores which ,if they do not have time to close during a period, will kill the cell (Wang et al, 2008). At last they can also replace the magnetic spherical microparticles which are currently used to capture and concentrate biological molecules. In this case it is their higher specific surface, which renders them more interesting than spherical particles.

References

Anilkumar P, Jayakannan M (2006) New renewable resource amphiphilic molecular design for size-controlled and highly ordered polyaniline nanofibers. *Langmuir* 22 (13): 5952-5957.

Bell RC, Karli JO, Vavreck AN, Zimmerman DT, Ngatu GT and Wereley NM (2008) Magnetorheology of submicron diameter iron microwires dispersed in silicon oil. *Smart Materials and Structures* 17: 015028.

Bell RC et al, (2007) Inluence of particle shape on the properties of magnetorheological fluids. *International Journal of Modern Physics B* 21: 5018.

Bossis G, Lacis S, Meunier A, Volkova O (2002) Magnetorheological Fluids. *Journal of Magnetism and Magnetic Materials* 252C: 224 – 228.

Bossis G, Lemaire E, Volkova O, Clercx H (1997) Yield stress in MR and ER fluids: a comparison between microscopic and macroscopic structural models. *Journal of Rheology* 41(3): 687-704

Choi HJ, Kim JW, Joo J, Kim BH (2001) Synthesis and electrorheology of emulsion intercalated PANI-clay nanocomposite. *Synthetic Metals* 121(1-3): 1325-1326.

Gonon P, Foulc JN, Atten P, and Boissy C (1999) Particle–particle interactions in electrorheological fluids based on surface conducting particles *Journal of Applied Physics* 86: 7160-7169.

Ginder JM, Davis LC, Elie LD (1996) Rheology of magnetorheological fluids: models and measurements *International Journal of Modern Physics* B (10): 3293–3303.

Jones TB (1995) *Electromechanics of particles.* Cambridge University Press p.119.

Kim YD, Song IC (2002) Electrorheological and dielectric properties of polypyrrole dispersions. *Journal of Materials Science* 37(23): 5051-5055.

Kuzhir P, Lopez-Lopez MT, Bossis G (2009) Magnetorheology of fiber suspension II. Theory. *Journal of Rheology* 53: 127-151.

Liu YD, Fang FF, Choi HJ, Seo Y (2011) Fabrication of semiconducting polyaniline/nano-silica nanocomposite particles and their enhanced electrorheological and dielectric characteristics. *Colloids and Surfaces a-Physicochemical and Engineering Aspects* 381(1-3): 17-22.

Lopez-Lopez MT, Vertelov G, Bossis G, et al. (2007) New magnetorheological fluids based on magnetic fibers. Journal of Materials Chemistry 17(36): 3839–3844.

Lopez-Lopez MT, Kuzhir P, Bossis G (2009) Magnetorheology of fiber suspension I. Experimental. *Journal of Rheology* 53:115-126.

Larson RG (1999) *The structure and rheology of complex fluids.* Oxford University Press.

Lim YT, Park JH, Park OO (2002) Improved electrorheological effect in polyaniline nanocomposite suspensions. *Journal of Colloid and Interface Science* 245(1): 198-203.

Marins JA, Giulieri F, Soares BG and Bossis G (2013) Hybrid polyaniline-coated sepiolite nanofibers for electrorheological fluid applications. *Synthetic Metals* 185-186: 9-16

J. Alves Marins, A. Mija, J. M. Pin, et al., Anisotropic Reinforcement of Epoxy-Based Nanocomposites with Aligned Magnetite-Sepiolite Hybrid Nanofiller, Composites Science Technology, 112, 34-41

Mendez-Garza J, Wang B, Madeira A, VierlingP Di-Giorgio C and Bossis G (2013) Synthesis and surface modification of spindle-type magnetic nanoparticles: gold coating and PEG functionalization *Journal of Biomaterials and Nanobiotechnology* 4:222-228 DOI 10.4236/jbnb.2013.43027

Ramos-Tejada MM, Espin MJ, Perea R, Delgado AV (2009) Electrorheology of suspensions of elongated goethite particles. *Journal of Non-Newtonian Fluid Mechanics* 159 (1-3).

Song DH, Lee HM, Lee KH, Choi HJ (2008) Intercalated conducting polyaniline-clay nanocomposites and their electrical characteristics. *Journal of Physics and Chemistry of Solids* 69(5-6): 1383-1385.

Vereda F, de Vicente J and Hidalgo-Alvarez R (2007) Influence of a magnetic field on the formation of magnetite particles via two precipitation methods. Langmuir 23(7): 3581–3589.

Volkova O (1998) *Study of the rheology of suspensions of magnetic particles.* PhD Thesis, University of Nice-Sophia Antipolis, France.

Wang B, Bienvenu C, Mendez-Garza J, et al. (2013) Necrosis of HepG2 cancer cells induced by the vibration of magnetic particles. Journal of Magnetism and Magnetic Materials 344: 193–201.

Wen W, Huang X, Yang S, Lu K and Sheng P (2003) The giant electrorheological effect in suspensions of nanoparticles. *Nature, Materials* 2(727).

Wu CW and Conrad H (1997) Dielectric and conduction effects in non-Ohmic electrorheological fluids. *Physical Revue E* 56: 5789-5797.

Wu J, Xu G, Cheng Y, Liu F, Guo J, Cui P (2012) The influence of high dielectric constant core on the activity of core–shell structure electrorheological fluid. *Journal of Colloid and Interface Science* 378: 36–43.

Yin J and Zhao X (2006) Titanate nano-whisker electrorheological fluid with high suspended stability and ER activity. *Nanotechnology* 17: 192–6.